JOC The Journal of Organic Chemistry

Article

pubs.acs.org/joc

Alkynylated Diazadioxaacenes: Syntheses and Properties

Manuel Schaffroth, Benjamin D. Lindner, Vladislav Vasilenko, Frank Rominger, and U. H. F. Bunz*

Organisch-Chemisches Institut, Universität Heidelberg, Im Neuenheimer Feld 270, 69120 Heidelberg

Supporting Information

ABSTRACT: We report the successful synthesis of a series of ethynylated dioxadiazaacenes and investigate their properties. We developed a modular Cu-based catalytic procedure to build up [1,4]dioxino[2,3-*b*]pyrazine motifs starting from only a few building blocks. TIPS-acetylene-substituted benzene-1,2-diol and naphthalene-2,3-diol were reacted with 2,3-dichloropyrazine, 2,3-dichloroquinoxaline, and 2,3-dichlorobenzoquinoxaline to give a set of six novel and well-soluble dioxadiazaacenes. Different reaction conditions for the coupling were tested. Copper catalysis is most effective and gave the best yield of dioxadiazaacenes. The resulting azaoxaacenes were characterized in terms of optical and electronic properties and crystal packing.

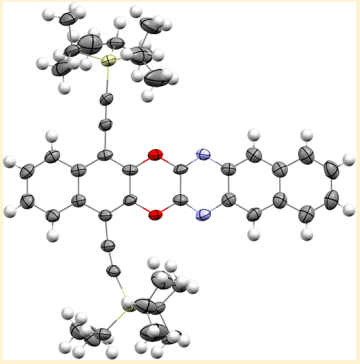

INTRODUCTION

Here we describe Pd- or Cu-catalyzed synthesis and photophysical, electrochemical, and structural characterization of a series of hitherto (almost) unknown heteroacene-derivatives featuring a [1,4]dioxino[2,3-*b*]pyrazine motif (Figure 1).

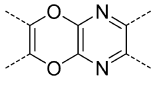

Figure 1. [1,4]Dioxino[2,3-*b*]pyrazine motif of the synthesized diazadioxaacenes.

Acenes as a class of compounds have garnered great attention for a variety of reasons including access to new structural motifs (graphene segments) and precursors of organic dyes due to their remarkable electronic properties.[1] Pentacene itself is a charge-carrier superstar but recently also pyrazine- or pyridine-carrying derivatives of pentacene (tetraazapentacene)[2−4] and also *N,N′*-dihydrodiazapentacenes[5] have been shown to be attractive charge-transporting materials. However, the potential evaluation of materials as effectors in organic electronic devices critically rests on their synthetic accessibility so that there is a constant pressure to make and evaluate new classes of compounds or perform "chemical mutagenesis" on the structures of known ones. One of the less investigated but potentially attractive classes of acene types are the diazadioxaacenes (Figure 1). To our knowledge, there are only a few derivatives of the larger diazadioxaacenes known, mainly 9,10-diaza-11,12-dioxatetracene **3** (Scheme 1).[6−9] These, however, are not very soluble and were not studied concerning their structural, optical, and electronic or electrochemical properties. Very recently, a related TIPS-triphenodioxazine compound was demonstrated to be a promising organic semiconductor.[10]

Scheme 1. Synthesis of 9,10-Diaza-11,12-dioxatetracene

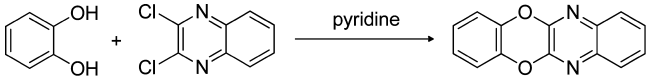

1 **2** **3**

Here, as an extension of known derivatives of acenes, we introduce a simple and efficient modular synthesis of azaoxatetracenes, -pentacenes, and -hexacenes and systematically evaluate their structural, electronic, and electrochemical properties.

RESULTS AND DISCUSSION

The synthesis of the target dioxadiazaacenes was planned by coupling diols such as **6** and **9** to halogenated pyrazine/quinoxaline derivatives. Diols **6** and **9** are unknown but can be made from the literature known dihalides **4** and **7** by Pd-catalyzed coupling to TIPS-acetylene to give the ethers **5** and **8**, respectively (Scheme 2).[11,12] Demethylation by BBr_3 at low temperature affords the diols **6** and **9** in overall yields of 60% for **6** and 40% for **9**.[13] The diols are (surprisingly) persistent at room temperature under laboratory conditions and can be stored for long periods of time in a freezer.

To test the coupling reactions, we treated **6** with dichloroquinoxaline (**2**) under different reaction conditions (Scheme 3). In a first experiment, we added base (Cs_2CO_3) and heated using microwave irridiation. The desired product **10** was formed in 21% yield after chromatography and crystallization. The yield of **10** increased to 37% upon addition of a Pd catalyst and a Buchwald-type ligand (RuPhos).[14] However, using copper iodide in the presence of picolinic acid

Received: January 15, 2013
Published: February 8, 2013

   dx.doi.org/10.1021/jo400092r | *J. Org. Chem.* 2013, 78, 3142−3150

Scheme 2. Synthesis of the Dihydroxyarenes 6 and 9

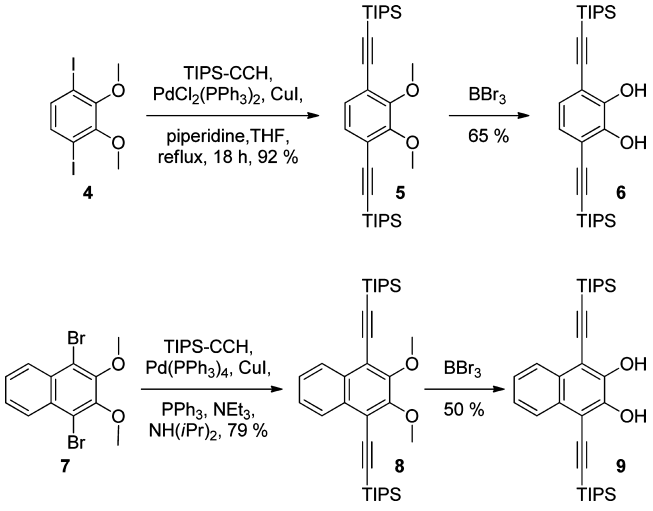

Scheme 3. Synthesis of the Diazadioxaacene 10 and Optimization of the Reaction Conditions

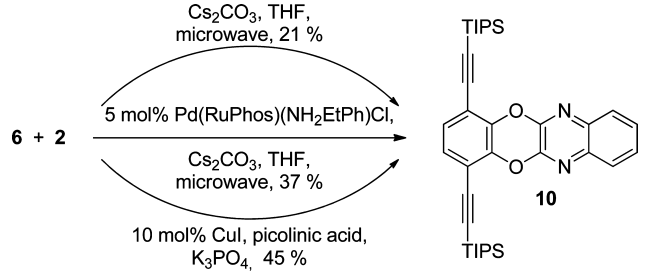

and K_3PO_4 as base is cheaper and worked even better, furnishing the coupling product **10** in 45% yield after chromatography.[15,16] Therefore, we selected this optimized method to perform all of the other coupling reactions.

In Scheme 4 we have applied the optimized conditions and coupled **6** and **9** in a modular fashion to **11**, **2**, and **15** to obtain the target molecules **12**–**14**, **16**, and **17** in satisfactory to good yields after chromatography and crystallization. In the solid state, these acene types are colorless to slightly greenish and show a blue to green fluorescence. In *n*-hexane all of them are blue fluorescent. The heteroacenes **16** and **17** show a distinct positive solvatochromism from blue to bright green (Figure 2).

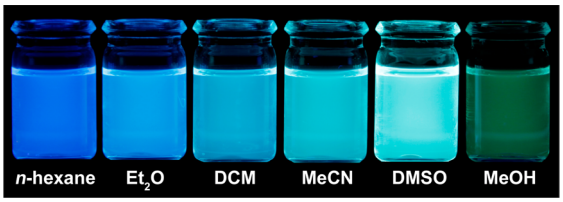

Figure 2. Photographs of the fluorescence of solutions (2×10^{-6} M) of **17** in different solvents (hand-held black light with an excitation of λ_{max} = 365 nm).

Optical Properties. Figure 3 displays the absorption spectra of the representative coupling products **10**, **14**, **16**, and **17**. In **10** and **16**, the dihydroxybenzene derivative **6** was the coupling partner, while for **14** and **17** catechol **9** served as the module. The absorption maximum of each compound is determined by the presence of the largest uninterrupted acene, i.e., the dioxine bridge is somewhat of a conjugative block, even though the whole system is formally conjugated. This is

Scheme 4. Synthesis of the Diazadioxaacenes 12–16

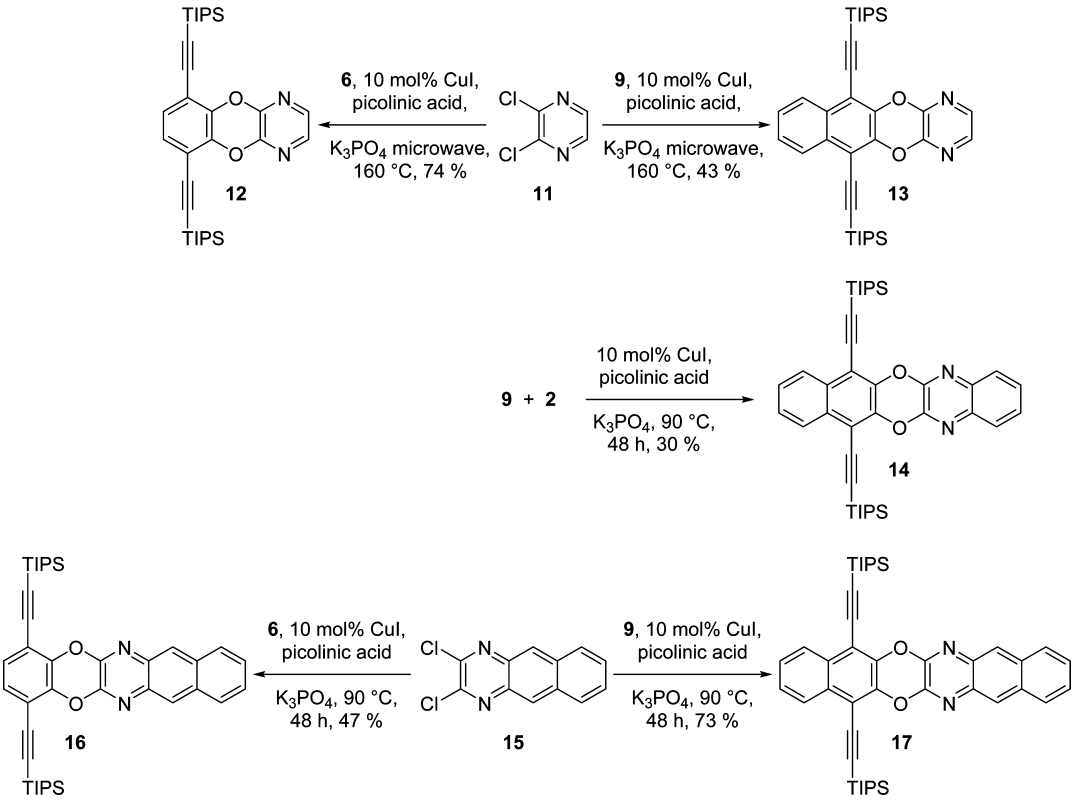

dx.doi.org/10.1021/jo400092r | J. Org. Chem. 2013, 78, 3142–3150

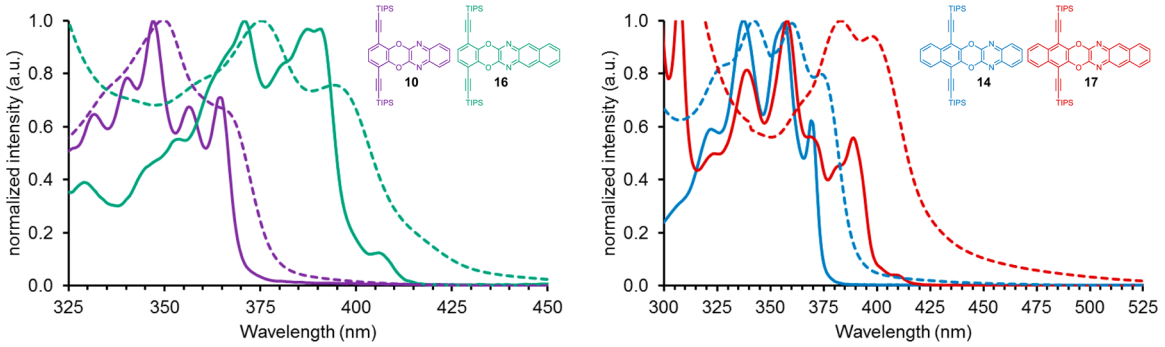

Figure 3. Normalized absorption spectra of **10** and **16** (left) and **14** and **17** (right) taken in *n*-hexane (solid line) and as a thin film (dashed line).

reminiscent of the isoelectronic *N,N′*-dihydrooligoazaacenes, which show a similar behavior. As a consequence, **16** and **17** have roughly the same λ_{max} in absorption and emission. While the diazadioxaacenes display a significant stokes shift (see Table 1), the compounds with the quinoxaline moiety **10** and **14**

Table 1. Photophysical Properties Recorded for the Diazadioxaacenes in Solution[a]

compd	abs λ_{max} (nm)	em λ_{max} (nm)	Stokes shift (cm^{-1})	$\Phi_f \pm 0.1$	τ_f[b] (ns)	ε (L mol^{-1} cm^{-1})
12	299	351	4955	0.35	*c*	80000
10	364	366	150	0.39	2.36	13000
16	387	408	1330	0.16	5.28	15800
13	355	369	1068	0.32	4.18	32200
14	369	370	74	0.51	2.59	29300
17	389	411	1376	0.13	5.25	24700

[a]All data were acquired in *n*-hexane as solvent. [b]Fluorescene lifetimes were measured in solution. [c]Compound **12** has almost no absorption at the wavelength of the excitation laser (376 nm). Thus, no reliable data could be obtained.

show almost no Stokes shifts. As an exception, **12** has a large Stokes shift of 4955 cm^{-1}, as it features no absorption maximum greater than 299 nm, although the absorption onset is at 350 nm (see the Supporting Information).

There is a small but significant red shift (≤5 nm) between the absorption spectra in solution and in thin film, but for **17** it extends to 33 nm. As the absorption peaks of **17** in thin film match peaks of the solution spectrum with lower intensity (at 369 and 389 nm), this red shift might refer to those vibronic fine structures. In contrast, the emission maxima show a substantial red shift, which reaches nearly 100 nm for compound **17** (Figure 4). This effect is due to the apparent interaction of the molecules in the solid state. The broad and featureless emission suggests that an excimer is formed. The fluorescence quantum yields were the highest for the quinoxaline containing compounds **10** and **14**, but the lowest for the products **16** and **17** having a benzoquinoxaline subunit. For the fluorescence lifetimes this order is inverted.

Solvatochromism. The absorption maximum of **17** did not change very much when screened from *n*-hexane to methanol. In contrast, the emission spectrum was quite sensitive to the solvent polarity (Figure 5, left). The plot (Figure 5, right) indicates that no specific interactions exist between the solvent and the dye, except for the polarizability as modeled by the Lippert−Mataga equation.[17] Only the value for methanol did not fit well to the plot, as the Lippert−Mataga model works best for aprotic solvents, where hydrogen bonding can be excluded.

MO Calculations and Aromaticity. If one looks at the diazadioxaacenes, there are two aromatic systems bridged by a formally antiaromatic 8π-system, the dioxine motif. These systems resemble the *N,N′*-dihydroazaacenes, which have been investigated in depth.[18−20] We have performed NICS(1)$_{zz}$ calculations on **10**, **12**−**14**, **16**, and **17** (Figure 6).[21−24] The geometry optimization was performed by TURBOMOLE employing B3LYP def2-TZVP, and a single-point energy calculation (Gaussian09, B3LYP 6-311++G**) followed.[25,26] The contributing 8π-dioxine rings all display positive NICS values, which range from 13.5 ppm for the largest computationally investigated acene to 17.6 ppm for the smallest, while all of the other rings show large negative NICS values. These heteroacenes are aromatic but have a somewhat diminished aromaticity as compared to that of the fully conjugated hydrocarbon congeners, similar to the situation described by

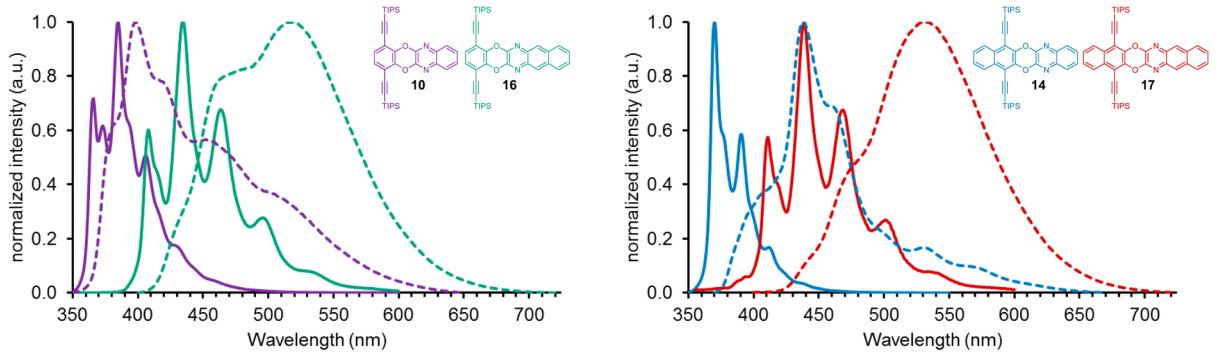

Figure 4. Normalized emission spectra of **10** and **16** (left) and **14** and **17** (right) taken in *n*-hexane (solid line) and as thin film (dashed line).

dx.doi.org/10.1021/jo400092r | J. Org. Chem. 2013, 78, 3142−3150

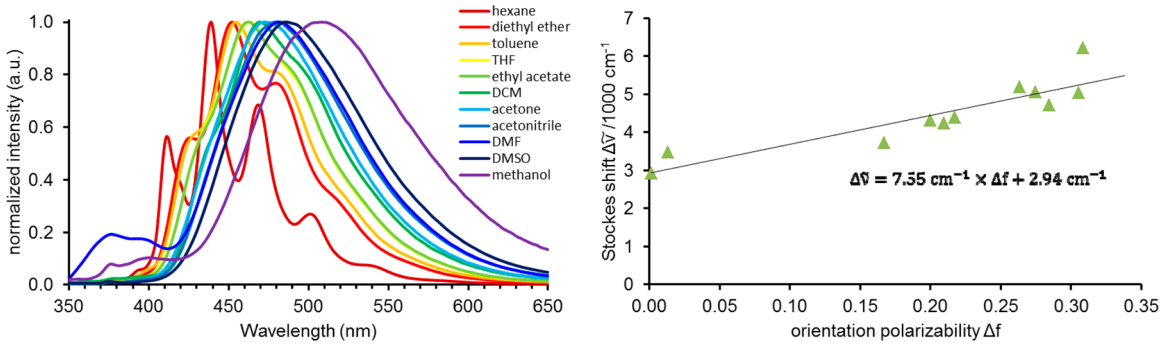

Figure 5. Normalized emission spectra of **17** in different solvents (left) and the corresponding Lippert–Mataga plot (right). For the calculation of the orientation polarizability Δf we used following formula: $\Delta f = (\varepsilon - 1)/(2\varepsilon + 1) - (n^2 - 1)/(2n^2 + 1)$, where ε is the relative permittivity and n the refractive index of the solvent.

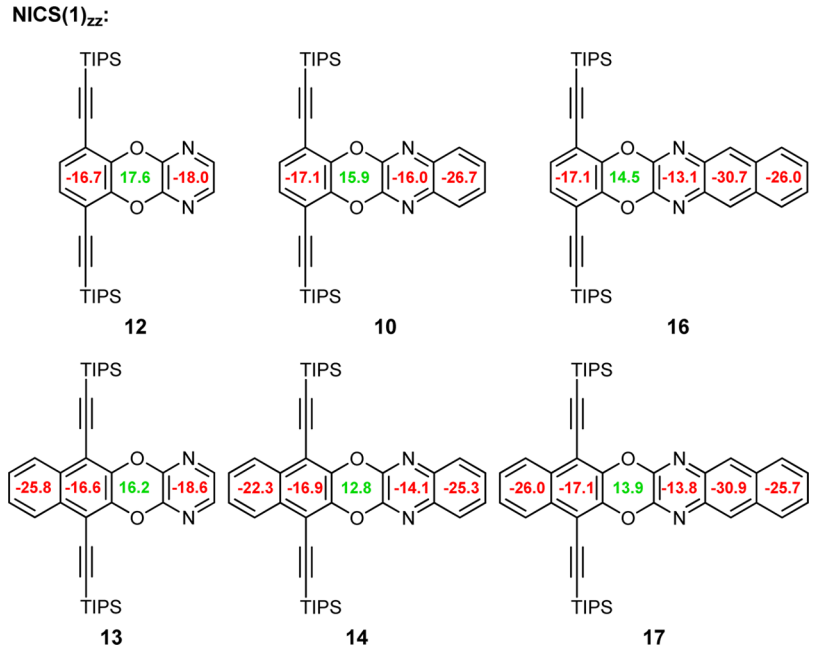

Figure 6. NICS(1)$_{zz}$ calculations (TURBOMOLE, B3LYP def2-TZVP//Gaussian09, B3LYP 6-311++G**).

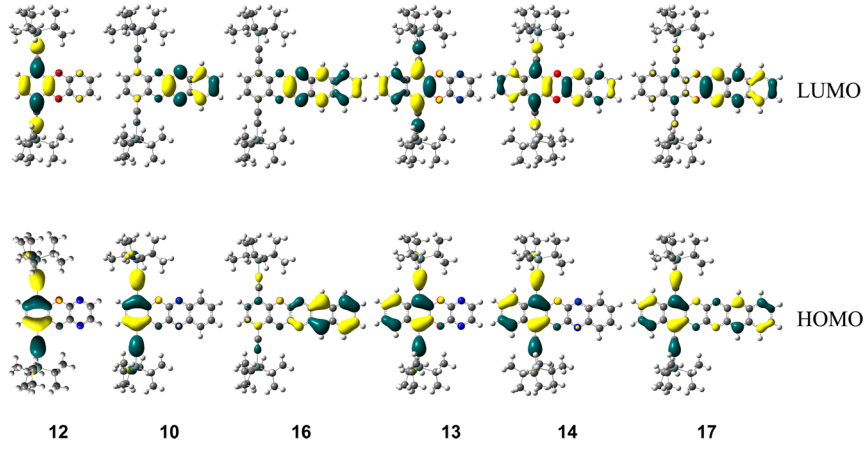

Figure 7. FMOs: LUMOs (top row) and HOMOs (bottom row) (calculated by TURBOMOLE, B3LYP def2-TZVP//Gaussian09, B3LYP 6-311++G**; for the citation see the Supporting Information).

us for the *N,N′*-dihydroazaacenes.[27] The synthesized diazadioxaacenes are stable and persistent, and do not experience any type of apparent destabilization by the presence of the 8π-system.

This separation of the molecules into two electronically separated "halves" is also obvious when looking at the FMOs (Figure 7). In most cases, the HOMOs and LUMOs are concentrated on *one* side of the molecule. The HOMOs are

dx.doi.org/10.1021/jo400092r | J. Org. Chem. 2013, 78, 3142–3150

mostly located on the side carrying the TIPS-ethynyl moiety, only for **16** is it located on the pyrazine side and for **17** it is delocalized on both sides. The LUMOs of **12** and **13** are also located on the TIPS-ethynyl side, while for **14** it is delocalized and for the other compounds it is situated on the pyrazine side. Without going into detail, a prerequisite for a substantial transfer integral and so a high charge carrier mobility, the HOMO (for hole transport) or the LUMO (for electron transport), respectively, should be delocalized as widely as possible. Thus, **14** features the only appropriate LUMO and **17** the best HOMO distribution of the whole set. These candidates might be interesting for possible applications in organic electronics.

Another important necessary criterion for good device performance is a low LUMO energy for n-channel transport or a high HOMO energy for p-channel transport. In Table 2,

Table 2. Calculated and Experimental HOMO−LUMO Gaps (Gas Phase) for the Synthesized Diazadioxaacenes and Pentacene for Comparison

compd	HOMO[a] (eV)	LUMO[a] (eV)	calcd gap (eV)	exptl gap[b] (eV)	$gap_{calc} - gap_{exp}$ (eV)
12	−6.31	−1.98	4.34	(339 nm) 3.66	0.68
10	−6.29	−2.21	4.08	(365 nm) 3.40	0.68
16	−6.04	−2.51	3.53	(402 nm) 3.08	0.45
13	−5.97	−2.26	3.71	(364 nm) 3.41	0.30
14	−5.94	−2.34	3.60	(367 nm) 3.38	0.22
17	−5.88	−2.56	3.31	(400 nm) 3.10	0.21
pentacene	−4.93	−2.74	2.20		

[a]Calculated by TURBOMOLE, B3LYP def2-TZVP//Gaussian09, B3LYP 6-311++G**. [b]Acquired from the intersection of the absorption and emission spectra.

the calculated energies and band gaps are shown and compared to experimental gaps acquired from the intersection of the absorption and emission spectra. The calculated gaps of the naphtho compounds **13**, **14**, and **17** fit quite well to the values obtained by experiment, while for the benzo compounds **12**, **10**, and **16** the values differ up to 0.68 eV. Overall, the LUMO energies are relatively high; therefore, these materials might not work well as electron-transport materials. However, the high-lying HOMO energies are suggestive that the diazadioxaacenes might be worth checking as hole transport materials, as in **17** the HOMO is only 1 eV lower in energy than that of pentacene.

Electrochemistry. Cyclic voltammetry shows that the coupling products display one reversible reduction potential versus ferrocene at −2.25 V (**13**), −2.20 V (**14**), −2.02 V (**16**), and −2.02 V (**17**). Reduction potentials of **10** and **12** were too near to the decomposition limit of the solvent to be determined. From these data, one can see that reduction of the pyrazine-containing subunit defines the reduction potential. Compound **13** displaying a pyrazine unit is less easily reduced than **16** or **17**, which incorporate a benzoquinoxaline unit. These results underscore the "split" nature of the diazadioxaacenes, which is determined by the separating oxygen bridges. For **17** we were also able to determine the first oxidation potential with a value of 0.64 V vs ferrocene. The measured reduction potentials and their calculated (B3LYP 6-311+G**) LUMO levels fit well into the master curve we have recently developed[19] to connect calculated LUMO levels with reduction potentials as measured by cyclic voltammetry (see Figure 8).

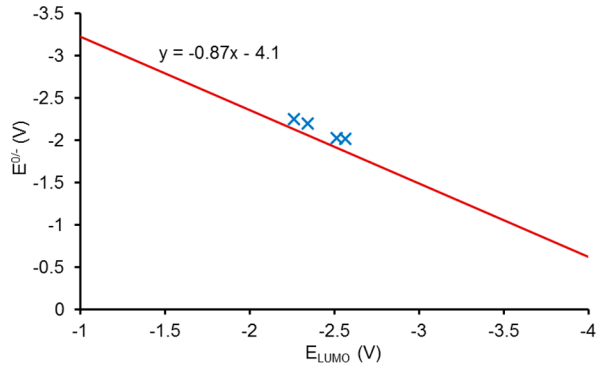

Figure 8. Comparison of the first reduction potentials to the calculated LUMO positions (TURBOMOLE, B3LYP def2-TZVP//Gaussian09, B3LYP 6-311+G**). The red line is taken from the master curve developed by Bunz et al.[19] connecting first reduction potentials with calculated LUMO levels. The blue spots are the values for the corresponding diazadioxaacenes.

Solid-State Structures. We obtained crystal structures of all six diazadioxaacenes (Figure 9). As expected, the measured bond lengths and angles fit well to those obtained from DFT calculations in the gas phase (TURBOMOLE, B3LYP def2-TZVP). Remarkably, the structures are very planar, with **14** showing the greatest angulation between the two aromatic moieties of 9.6° at the dioxine ring (Figure 10, bottom right).

Because of crystal packing effects, the ethynyl units are often bent in TIPS-ethynylated acenes and heteroacenes.[19,28] In **14**, **16**, and **17**, the bending of the alkynes is particularly obvious. The packing of the azaoxaacenes is different for each. Compound **12** forms one-dimensional stacks but does not show much overlap of the acene backbone becaue of the TIPS substituents. So does **10**, but with more overlap and units of two molecules, inversely superimposed. Compound **16** forms a herringbone motif with plane distances of 3.32, 3.51, 3.36 Å and 3.40 Å, respectively (Figure 10). These plane distances might be small enough for an efficient charge transport. Compound **13** forms dimers at the pyrazine units with a CH−N bond length of 2.69 Å. The dimers are arranged in a herringbone motif with only small overlap. The kinked **14** forms a brickwall motif, while **17** features a herringbone motif. One stack shows inversely superimposed pairs of molecules with plane distances of 3.36 and 3.37 Å, and the other moiety has equally oriented molecules with a plane distance of 3.39 Å. In addition to spread out FMOs and appropriate energy levels, a good overlap of the molecules in the solid phase is critical to an efficient charge transport as it should increase the overlap integral.[29] Azaoxaacenes **14**, **16**, and **17** fulfill this condition to a good degree and will be investigated in TFT-type devices.

CONCLUSION

We have produced a series of hitherto unknown, substituted, stable, and soluble diazadioxaacenes by a modular coupling process of aromatic *ortho*-diols to dichloropyrazines, -quinoxalines, and -benzoquinoxalines. The best method for their modular synthesis is the cheap, copper-catalyzed, base-promoted reaction developed by Buchwald et al. superior to

dx.doi.org/10.1021/jo400092r | J. Org. Chem. 2013, 78, 3142−3150

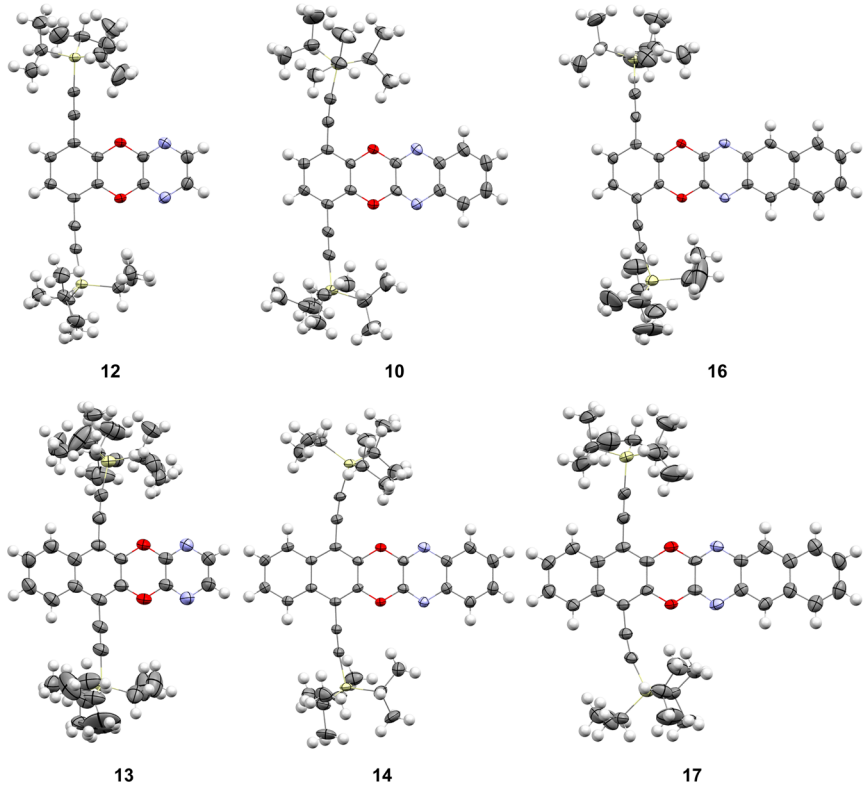

Figure 9. Crystal structures of **12**, **10**, **16**, **13**, **14**, and **17**.

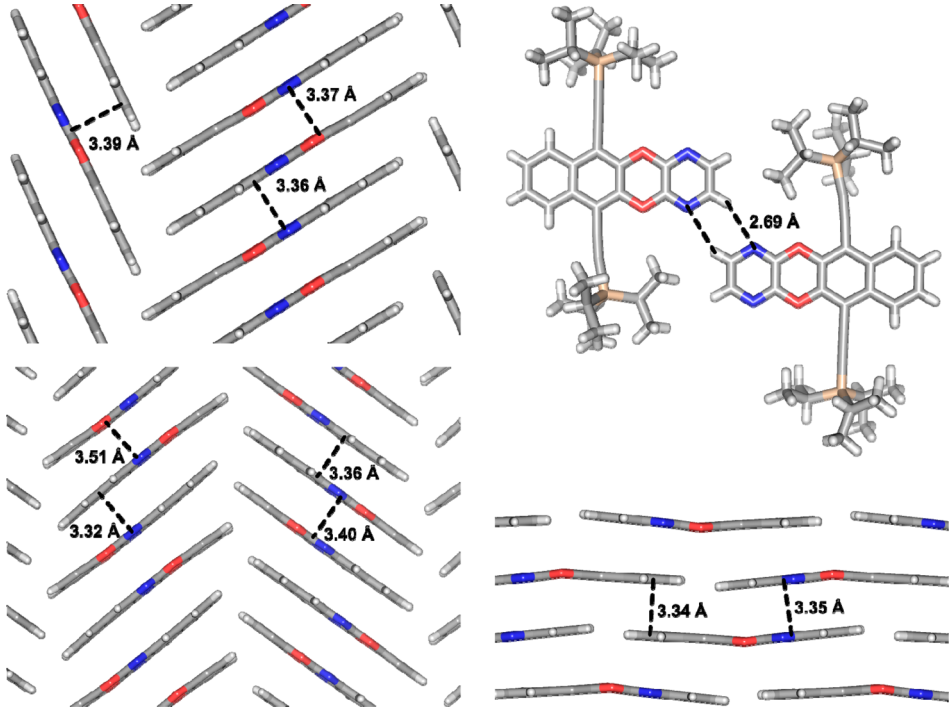

Figure 10. Herringbone motif of **16** (top, left), dimer of **13** (top, right), the herringbone motif of **17** (bottom, left), and brickwall motif of kinked **14** (bottom, right). Where necessary for a better overview, the ethynyl side chains were hidden.

either that uses only base- or even Pd-catalyzed processes.[15] The obtained heteroacenes are persistent and stable under laboratory conditions and display promising crystal packings. Despite the formally antiaromatic dioxine ring, they overall exhibit aromaticity, albeit somewhat reduced. The diminished conjugation at the dioxine ring often causes a localization of the FMOs on one-half of the molecules, and consequently relatively high LUMO and low HOMO energies result. In contrast to the fully conjugated N-heteroacenes, these molecules could prove to work as a p-channel material. Here, especially **17** might be a promising candidate due to its spread out HOMO distribution, high HOMO level (oxidized at 0.64 V

dx.doi.org/10.1021/jo400092r | J. Org. Chem. 2013, 78, 3142−3150

vs ferrocene), and good crystal packing. In the future, we will investigate larger diazadioxaacenes in organic thin film transistors.

EXPERIMENTAL SECTION

Quantum yields were measured relative to quinine sulfate in dilute sulfuric acid. Time-correlated single photon counting lifetime measurements were made with a pulsed laser diode. Computational studies were carried out using DFT calculations on a Turbomole 6.3.1 or a Gaussian09 platform. Geometry optimization was found by B3LYP functional and def2-TZVP basis set. Using this geometry, FMO energies were assigned on single point approach by employing B3LYP/6-311++G**. Electrochemical measurements were performed using 0.1 M n-Bu_4NPF_6 in dry THF or DCM as electrolyte solution. Potentials were determined using cyclic voltammetry at 40 mV s^{-1} using a platinum working electrode and a platinum/titanium wire auxiliary electrode. Ferrocene was used as an internal reference.

1,4-Diiodo-2,3-dimethoxybenzene (4). Compound **4** was synthesized according to the procedure described by Zhu and Swager:[11] R_f = 0.65 (PE/EA = 9:1); ^{1}H NMR (300 MHz, $CDCl_3$, 25 °C) δ = 3.87 (s, 6H), 7.24 (s, 2H).

[(2,3-Dimethoxybenzene-1,4-diyl)diethyne-2,1-diyl]bis[tri(prop-2-yl)silane] (5). Under an atmosphere of argon, **4** (4.00 g, 10.3 mmol), piperidine (4.39 g, 5.09 mL, 51.5 mmol, 5 equiv), $Pd(PPh_3)_2Cl_2$ (361 mg, 515 μmol, 5 mol %), and CuI (98.1 mg, 515 μmol, 5 mol %) were dissolved in dry THF (50 mL), and the mixture was degassed three times (freeze−thaw method). After slow addition of TIPS-acetylene (5.64 g, 6.94 mL, 30.9 mmol, 3 equiv) the solution was stirred under reflux for 18 h. The mixture was filtered through Celite and concentrated. Flash chromatography (petroleum ether/CH_2Cl_2 10:1) gave **5** as a colorless liquid (4.73 g, 9.47 mmol, 92%): R_f = 0.64 (PE/EA = 20:1); ^{1}H NMR (600 MHz, $CDCl_3$, 25 °C) δ = 1.10−1.17 (m, 42H), 3.95 (s, 6H), 7.08 (s, 2H); ^{13}C {^{1}H} NMR (150 MHz, $CDCl_3$, 25 °C) δ = 11.4, 18.7, 61.1, 97.1, 102.4, 119.2, 128.3, 154.7; IR ν = 2941, 2890, 2863, 2155, 1459, 1401, 1230, 1066, 1030, 995, 922, 881, 818, 779, 676, 656, 589, 479, 457, 446; HR-MS (ESI-FT-ICR) m/z calcd for $C_{30}H_{51}O_2Si_2$ $[M + H]^+$ 499.34221, found 499.34227.

3,6-Bis[[tri(prop-2-yl)silyl]ethynyl]benzene-1,2-diol (6). Under an atmosphere of nitrogen, **5** (4.72 g, 9.46 mmol) was dissolved in dry CH_2Cl_2 (50 mL) at −78 °C. After slow addition of BBr_3 (3.56 g, 1.35 mL, 14.2 mmol, 1.5 equiv) the solution was stirred under warming to rt for 1.5 h. Then ice−water was added, and the mixture was stirred for 30 min. After extraction with CH_2Cl_2, the organic phase was washed with water twice, dried over Na_2SO_4, and concentrated. Flash chromatography (petroleum ether/ethyl acetate 100:1) gave **6** as a colorless solid (2.88 g, 6.12 mmol, 65%): R_f = 0.58 (PE/EA = 9:1); mp 122 °C; ^{1}H NMR (600 MHz, $CDCl_3$, 25 °C) δ = 1.12−1.16 (m, 42H), 5.74 (s, 2H), 6.87 (s, 2H); ^{13}C {^{1}H} NMR (150 MHz, $CDCl_3$, 25 °C) δ = 11.2, 18.7, 99.7, 100.7, 111.1, 123.0, 144.8; IR ν = 3502, 2942, 2863, 2146, 1614, 1452, 1303, 1230, 1205, 997, 945, 882, 803, 785, 678, 640, 626, 578, 531, 499, 460, 446, 404; HR-MS (ESI-FT-ICR) m/z calcd for $C_{28}H_{46}NaO_2Si_2$ $[M + Na]^+$ 493.29285, found 493.29274.

1,4-Dibromo-2,3-dimethoxynaphthalene (7). 2,3-Dimethoxynaphthalene (1.00g, 5.31 mmol) was dissolved in glacial acetic acid (7 mL). After slow addition of a solution of Br_2 (1.69 g, 0.54 mL, 10.6 mmol, 2 equiv) in glacial acetic acid (3 mL), the solution was stirred in the dark at rt for 24 h. Then a saturated solution of $Na_2S_2O_3$ was added, and the mixture was extracted with CH_2Cl_2. The organic phase was washed with a saturated solution of $NaHCO_3$ and twice with water, dried over Na_2SO_4, and concentrated. Flash chromatography (petroleum ether/ethyl acetate 100:1) gave **7** as a colorless solid (1.48 g, 4.28 mmol, 81%): R_f = 0.57 (PE/EA = 9:1); ^{1}H NMR (300 MHz, $CDCl_3$, 25 °C) δ = 4.01 (s, 6H), 7.52−7.61 (m, 2H), 8.20−8.28 (m, 2H).

[(2,3-Dimethoxynaphthalene-1,4-diyl)diethyne-2,1-diyl]bis[tri(prop-2-yl)silane] (8). Under an atmosphere of nitrogen, **7** (4.39 g, 12.7 mmol), $Pd(PPh_3)_4$ (294 mg, 254 μmol, 2 mol %), PPh_3 (133 mg, 508 μmol, 4 mol %), and CuI (96.7 mg, 508 μmol, 4 mol %) were dissolved in dry NEt_3 (65 mL) and $NH(i\text{-}Pr)_3$ (25 mL). The mixture was degassed three times (freeze−thaw method). After slow addition of TIPS-acetylene (6.95 g, 8.55 mL, 38.1 mmol, 3 equiv), the solution was stirred under reflux for 16 h. The mixture was filtered through Celite, extracted with CH_2Cl_2, and washed with water twice and with a saturated solution of NH_4Cl. The organic phase was dried over Na_2SO_4 and concentrated. Flash chromatography (petroleum ether/ethyl acetate 500:1 to 100:1) gave **8** as a colorless solid (5.48 g, 9.98 mmol, 79%): R_f = 0.82 (PE/EA = 9:1); mp 39 °C; ^{1}H NMR (300 MHz, $CDCl_3$, 25 °C) δ = 1.19−1.23 (m, 42H), 4.05 (s, 6H), 7.48−7.53 (m, 2H), 8.25−8.30 (m, 2H); ^{13}C {^{1}H} NMR (75 MHz, $CDCl_3$, 25 °C) δ = 11.5, 18.8, 61.5, 100.3, 102.8, 115.0, 125.9, 126.4, 131.1, 155.2; IR ν = 2941, 2890, 2864, 2144, 1457, 1376, 1246, 1043, 1016, 995, 956, 881, 766, 712, 677, 574, 504, 458; HR-MS (ESI-FT-ICR) m/z calcd for $C_{34}H_{53}O_2Si_2$ $[M + H]^+$ 549.35786, found 549.35791.

1,4-Bis[[tri(prop-2-yl)silyl]ethynyl]naphthalene-2,3-diol (9). Under an atmosphere of nitrogen, **8** (549 g, 1.00 mmol) was dissolved in dry CH_2Cl_2 (5 mL) at −78 °C. After slow addition of BBr_3 (501 mg, 190 μL, 2.00 mmol, 2 equiv), the solution was stirred at −78 °C for 45 min and afterward under warming to rt for 1 h. Then ice−water was added, and the mixture was stirred for 1 h. After extraction with CH_2Cl_2, the organic phase was washed with water twice, dried over Na_2SO_4, and concentrated. Flash chromatography (petroleum ether/ethyl acetate 200:1) gave **6** as a colorless solid (251 mg, 482 μmol, 48%): R_f = 0.53 (PE/EA = 9:1); mp 137 °C under decompostion; ^{1}H NMR (600 MHz, $CDCl_3$, 25 °C) δ = 1.18−1.23 (m, 42H), 6.17 (s, 2H), 7.43−7.47 (m, 2H), 8.07−8.11 (m, 2H); ^{13}C {^{1}H} NMR (150 MHz, $CDCl_3$, 25 °C) δ = 11.3, 18.8, 98.8, 104.9, 105.4, 125.2, 125.6, 128.4, 146.5; IR ν = 3504, 3458, 2941, 2863, 2148, 1513, 1460, 1442, 1381, 1287, 1254, 1221, 1194, 1153, 1019, 996, 943, 881, 860, 761, 670, 573, 507, 467, 435, 415, 405; HR-MS (ESI-FT-ICR) m/z calcd for $C_{32}H_{49}O_2Si_2$ $[M + H]^+$ 521.32656, found 521.32662.

1,4-Bis[[tri(prop-2-yl)silyl]ethynyl][1,4]benzodioxino[2,3-*b*]quinoxaline (10). (i) Under an atmosphere of argon, **6** (50.0 mg, 106 μmol), **2** (21.1 mg, 106 μmol, 1 equiv), and Cs_2CO_3 (104 mg, 318 μmol, 3 equiv) were dissolved in dry THF (2 mL) in a 10 mL microwave tube. In the microwave reactor, the mixture was stirred at 150 °C for 2 h. The mixture was purified by flash chromatography (petroleum ether/ethyl acetate 200:1) to obtain **10** as a colorless solid (13.0 mg, 21.8 μmol, 21%).

(ii) Under an atmosphere of argon, **6** (50.0 mg, 106 μmol), **2** (21.1 mg, 106 μmol, 1 equiv), Pd(RuPhos)(NH_2EtPh)Cl (3.86 mg, 5.30 μmol, 5 mol %), RuPhos (2.47 mg, 5.30 μmol, 5 mol %), and Cs_2CO_3 (104 mg, 318 μmol, 3 equiv) were dissolved in dry THF (2 mL) in a 10 mL microwave tube. In the microwave reactor, the mixture was stirred at 150 °C for 2 h. The mixture was purified by flash chromatography (petroleum ether/ethyl acetate 200:1) to obtain **10** as a colorless solid (23.5 mg, 39.4 μmol, 37%).

(iii) Under an atmosphere of nitrogen, **6** (50.0 mg, 106 μmol), **2** (21.1 mg, 106 μmol, 1 equiv), CuI (2.02 mg, 10.6 μmol, 10 mol %), picolinic acid (2.61 mg, 21.2 μmol, 20 mol %), and K_3PO_4 (90.0 mg, 424 μmol, 4 equiv) were dissolved in dry DMSO (2 mL). The mixture was stirred at 90 °C for 24 h. After dilution with diethyl ether and washing with water, the organic phase was dried over Na_2SO_4 and concentrated. The mixture was purified by flash chromatography (petroleum ether/ethyl acetate 300:1) to obtain **10** as a colorless solid (28.5 mg, 47.7 μmol, 45%): R_f = 0.64 (PE/EA = 9:1); mp 146 °C; ^{1}H NMR (300 MHz, $CDCl_3$, 25 °C) δ = 1.14−1.22 (m, 42H), 7.10 (s, 2H), 7.54−7.62 (m, 2H), 7.79−7.86 (m, 2H); ^{13}C {^{1}H} NMR (75 MHz, $CDCl_3$, 25 °C) δ = 11.3, 18.7, 99.5, 100.6, 113.1, 127.6, 128.3, 128.8, 139.5, 141.9, 144.1; IR ν = 2942, 2890, 2864, 2157, 1420, 1372, 1330, 1231, 1167, 1141, 1052, 1019, 995, 881, 794, 759, 748, 675, 658, 616, 580, 447; UV−vis λ_{max} (hexane) 364 nm; ε(364 nm)= 13000 $L{\cdot}mol^{-1}{\cdot}cm^{-1}$; fluorescence λ_{max} (hexane) 366 nm; HR-MS (ESI-FT-ICR) m/z calcd for $C_{36}H_{49}N_2O_2Si_2$ $[M + H]^+$ 597.33271, found 597.33395.

6,9-Bis[[tri(prop-2-yl)silyl]ethynyl][1,4]benzodioxino[2,3-*b*]pyrazine (12). Under an atmosphere of argon, **6** (150 mg, 319 μmol),

dx.doi.org/10.1021/jo400092r | J. Org. Chem. 2013, 78, 3142−3150

11 (47.5 mg, 319 μmol, 1 equiv), CuI (6.08 mg, 31.9 μmol, 10 mol %), picolinic acid (7.85 mg, 63.8 μmol, 20 mol %), and K_3PO_4 (272 mg, 1.28 mmol, 4 equiv) were dissolved in a mixture of dry dimethoxyethan (2 mL) and dry toluene (2 mL) in a 10 mL microwave tube. In the microwave reactor the mixture was stirred at 160 °C for 4 h. After dilution with diethyl ether and washing with water, the organic phase was dried over $MgSO_4$ and concentrated. The mixture was purified by flash chromatography (petroleum ether/ethyl acetate 250:1) to obtain **12** as a colorless solid (130 mg, 237 μmol, 74%): R_f = 0.55 (PE/EA = 9:1); mp 155 °C; ^{1}H NMR (400 MHz, $CDCl_3$, 25 °C) δ = 1.13−1.20 (m, 42H), 7.04 (s, 2H), 7.83 (s, 2H); ^{13}C {^{1}H} NMR (100 MHz, $CDCl_3$, 25 °C) δ = 11.3, 18.7, 99.5, 100.3, 113.0, 128.3, 137.8, 142.4, 146.0; IR ν = 2942, 2890, 2864, 2157, 1581, 1462, 1410, 1388, 1303, 1189, 1162, 1037, 1001, 881, 816, 783, 695, 675, 660, 627, 585, 506, 470, 460, 417, 405; UV−vis λ_{max} (hexane) 299 nm; ε(299 nm)= 80000 L·mol^{-1}·cm^{-1}; fluorescence λ_{max} (hexane) 351 nm; HR-MS (ESI-FT-ICR) *m*/*z* calcd for $C_{32}H_{47}N_2O_2Si_2$ $[M + H]^+$ 547.31706, found 547.31779.

6,11-Bis[[tri(prop-2-yl)silyl]ethynyl]naphtho[2′,3′:5,6][1,4]dioxino[2,3-*b*]pyrazine (13). Under an atmosphere of argon, **9** (100 mg, 192 μmol), **11** (28.6 mg, 192 μmol, 1 equiv), CuI (3.66 mg, 19.2 μmol, 10 mol %), picolinic acid (4.73 mg, 38.4 μmol, 20 mol %), and K_3PO_4 (163 mg, 768 μmol, 4 equiv) were dissolved in a mixture of dry dimethoxyethane (2 mL) and dry toluene (2 mL) in a 10 mL microwave tube. In the microwave reactor, the mixture was stirred at 160 °C for 2 h. After dilution with diethyl ether and washing with water, the organic phase was dried over $MgSO_4$, and concentrated. The mixture was purified by flash chromatography (petroleum ether/ethyl acetate 250:1) to obtain **12** as a colorless solid (130 mg, 237 μmol, 43%): R_f = 0.57 (PE/EA = 9:1); mp 176 °C; ^{1}H NMR (600 MHz, $CDCl_3$, 25 °C) δ = 1.19−1.30 (m, 42H), 7.51−7.55 (m, 2H), 7.90 (s, 2H), 8.22−8.27 (m, 2H); ^{13}C {^{1}H} NMR (150 MHz, $CDCl_3$, 25 °C) δ = 11.4, 18.8, 97.7, 105.9, 108.5, 126.1, 127.2, 130.6, 137.8, 142.4, 144.5; IR ν = 2941, 2890, 2863, 2162, 2140, 1598, 1460, 1430, 1403, 1367, 1351, 1337, 1304, 1248, 1191, 1166, 1032, 1016, 993, 960, 881, 850, 761, 746, 676, 664, 652, 605, 581, 496, 470, 460, 418; UV−vis λ_{max} (hexane) 355 nm; ε(355 nm) = 32200 L·mol^{-1}·cm^{-1}; fluorescence λ_{max} (hexane) 369 nm; HR-MS (ESI-FT-ICR) *m*/*z* calcd for $C_{36}H_{49}N_2O_2Si_2$ $[M + H]^+$ 597.33271, found 597.33393.

7,12-Bis[[tri(prop-2-yl)silyl]ethynyl]naphtho[2′,3′:5,6][1,4]dioxino[2,3-*b*]quinoxaline (14). Under an atmosphere of nitrogen, **9** (156 mg, 300 μmol), **2** (59.7 mg, 300 μmol, 1 equiv), CuI (5.71 mg, 30.0 μmol, 10 mol %), picolinic acid (7.39 mg, 60.0 μmol, 20 mol %), and K_3PO_4 (255 mg, 1.20 mmol, 4 equiv) were dissolved in dry DMSO (4 mL). The mixture was stirred at 90 °C for 24 h. After dilution with diethyl ether and washing with water, the organic phase was dried over Na_2SO_4 and concentrated. The mixture was purified by flash chromatography (petroleum ether/ethyl acetate 500:1) to obtain **14** as a yellow solid (57.6 mg, 89.0 μmol, 30%): R_f = 0.65 (PE/EA = 9:1); mp 225 °C dec; ^{1}H NMR (600 MHz, $CDCl_3$, 25 °C) δ = 1.24−1.32 (m, 42H), 7.53−7.58 (m, 2H), 7.59−7.63 (m, 2H), 7.86−7.90 (m, 2H), 8.26−8.31 (m, 2H); ^{13}C {^{1}H} NMR (150 MHz, $CDCl_3$, 25 °C) δ = 11.4, 18.8, 97.7, 106.2, 108.6, 126.2, 127.2, 127.7, 128.8, 130.6, 139.5, 141.9, 143.6; IR ν = 2941, 2891, 2864, 2155, 2137, 1415, 1395, 1371, 1338, 1329, 1254, 1232, 1039, 985, 882, 766, 758, 713, 675, 659, 605, 447; UV−vis λ_{max} (hexane) 369 nm; ε(369 nm)= 29300 L·mol^{-1}·cm^{-1}; fluorescence λ_{max} (hexane): 670 nm; HR-MS (ESI-FT-ICR) *m*/*z* calcd for $C_{40}H_{51}N_2O_2Si_2$ $[M + H]^+$ 647.34836, found 647.34969.

1,4-Bis[[tri(prop-2-yl)silyl]ethynyl][1,4]benzodioxino[2,3-*b*]benzo[*g*]quinoxaline (16). Under an atmosphere of nitrogen, **6** (150 mg, 319 μmol), **15** (79.5 mg, 319 μmol, 1 equiv), CuI (6.08 mg, 31.9 μmol, 10 mol %), picolinic acid (7.85 mg, 63.8 μmol, 20 mol %), and K_3PO_4 (272 mg, 1.28 mmol, 4 equiv) were dissolved in dry DMSO (4 mL). The mixture was stirred at 90 °C for 48 h. After dilution with diethyl ether and washing with water, the organic phase was dried over Na_2SO_4 and concentrated. The mixture was purified by flash chromatography (petroleum ether/ethyl acetate 500:1) to obtain **16** as a yellow solid (96.1 mg, 149 μmol, 47%): R_f = 0.69 (PE/EA = 9:1); mp 280 °C dec; ^{1}H NMR (500 MHz, $CDCl_3$, 25 °C) δ = 1.19−1.23 (m, 42H), 7.13 (s, 2H), 7.50−7.55 (m, 2H), 7.98−8.03 (m, 2H), 8.34 (s, 2H); ^{13}C {^{1}H} NMR (125 MHz, $CDCl_3$, 25 °C) δ = 11.4, 18.7, 99.4, 100.8, 113.2, 125.7, 126.5, 128.1, 128.3, 133.3, 136.8, 141.6, 144.1; IR ν = 2942, 2890, 2864, 2154, 1433, 1395, 1362, 1279, 1169, 1053, 1017, 876, 768, 744, 675, 660, 627, 596, 470, 433; UV−vis λ_{max} (hexane) 387 nm; ε(387 nm)= 15800 L·mol^{-1}·cm^{-1}; fluorescence λ_{max} (hexane) 408 nm; HR-MS (ESI-FT-ICR) *m*/*z* calcd for $C_{40}H_{51}N_2O_2Si_2$ $[M + H]^+$ 647.34836, found 647.35257. Anal. Calcd for $C_{40}H_{50}N_2O_2Si_2$: C, 74.25; H, 7.79; N, 4.33. Found: C, 74.07; H, 7.67; N, 4.14.

5,16-Bis[[tri(prop-2-yl)silyl]ethynyl]benzo[*g*]naphtho[2′,3′:5,6][1,4]dioxino[2,3-*b*]quinoxaline (17). Under an atmosphere of nitrogen, **9** (156 mg, 300 μmol), **15** (74.7 mg, 300 μmol, 1 equiv), CuI (5.71 mg, 30.0 μmol, 10 mol %), picolinic acid (7.39 mg, 60.0 μmol, 20 mol %), and K_3PO_4 (255 mg, 1.20 mmol, 4 equiv) were dissolved in dry DMSO (4 mL). The mixture was stirred at 90 °C for 48 h. After dilution with diethyl ether and washing with water, the organic phase was dried over Na_2SO_4 and concentrated. The mixture was purified by flash chromatography (petroleum ether/ethyl acetate 500:1) to obtain **17** as a yellow solid (152 mg, 218 μmol, 73%): R_f = 0.71 (PE/EA = 9:1); mp 374 °C dec; ^{1}H NMR (400 MHz, $CDCl_3$, 25 °C) δ = 1.25−1.32 (m, 42H), 7.48−7.54 (m, 2H), 7.55−7.61 (m, 2H), 7.99−8.05 (m, 2H), 8.28−8.34 (m, 2H), 8.40 (s, 2H); ^{13}C {^{1}H} NMR (100 MHz, $CDCl_3$, 25 °C) δ = 11.5, 18.9, 97.7, 106.4, 108.7, 125.8, 126.2, 126.5, 127.3, 128.2, 130.6, 133.3, 136.8, 141.6, 143.7; IR ν = 2941, 2890, 2864, 2164, 2137, 1425, 1396, 1361, 1346, 1280, 1168, 1139, 1106, 1037, 989, 877, 761, 740, 672, 660, 583, 499, 489, 471, 461, 432, 420, 408; UV−vis λ_{max} (hexane) 389 nm; ε(389 nm) = 24700 L·mol^{-1}·cm^{-1}; fluorescence λ_{max} (hexane): 411 nm; HR-MS (ESI-FT-ICR) *m*/*z* calcd for $C_{44}H_{53}N_2O_2Si_2$ $[M + H]^+$ 697.36401, found 697.36422.

■ ASSOCIATED CONTENT

Supporting Information

Copies of NMR spectra, full scaled absorption and emission spectra, further information about the computational calculations, and X-ray data (cif). This material is available free of charge via the Internet at http://pubs.acs.org.

■ AUTHOR INFORMATION

Corresponding Author

*E-mail: uwe.bunz@oci.uni-heidelberg.de.

Notes

The authors declare no competing financial interest.

■ ACKNOWLEDGMENTS

We thank the Struktur and Innovation Fonds of the State of Baden-Württemberg for generous support.

■ REFERENCES

(1) Anthony, J. E. *Angew. Chem. Int Ed.* **2008**, *47*, 452−483.
(2) Miao, S.; Appleton, A. L.; Berger, N.; Barlow, S.; Marder, S. R.; Hardcastle, K. I.; Bunz, U. H. F. *Chem.—Eur. J.* **2009**, *15*, 4990−4993.
(3) Wang, C.; Liang, Z.; Liu, Y.; Wang, X.; Zhao, N.; Miao, Q.; Hu, W.; Xu, J. *J. Mater. Chem.* **2011**, *21*, 15201−15204.
(4) Liang, Z.; Tang, Q.; Xu, J.; Miao, Q. *Adv. Mater. (Weinheim, Ger.)* **2011**, *23*, 1535−1539.
(5) Miao, Q.; Nguyen, T.-Q.; Someya, T.; Blanchet, G. B.; Nuckolls, C. *J. Am. Chem. Soc.* **2003**, *125*, 10284−10287.
(6) Kehrmann, F.; Bener, C. *Helv. Chim. Acta* **1925**, *8*, 16−20.
(7) Wolf, R.; Marvel, C. S. *J. Polym. Sci. Part A-1: Polym. Chem.* **1969**, *7*, 2481−2491.
(8) Ames, D. E.; Ward, R. J. *J. Chem. Soc., Perkin Trans. 1* **1975**, 534−538.
(9) Lee, H. H.; Denny, W. A. *J. Chem. Soc., Perkin Trans. 1* **1990**, 1071−1074.

(10) Nicolas, Y.; Castet, F.; Devynck, M.; Tardy, P.; Hirsch, L.; Labrugère, C.; Allouchi, H.; Toupance, T. *Org. Electron.* **2012**, *13*, 1392−1400.
(11) Zhu, Z.; Swager, T. M. *Org. Lett.* **2001**, *3*, 3471−3474.
(12) Zhao, Y.-L.; Liu, L.; Zhang, W.; Sue, C.-H.; Li, Q.; Miljanić, O. Š.; Yaghi, O. M.; Stoddart, J. F. *Chem.—Eur. J.* **2009**, *15*, 13356−13380.
(13) Vickery, E. H.; Pahler, L. F.; Eisenbraun, E. J. *J. Org. Chem.* **1979**, *44*, 4444−4446.
(14) Surry, D. S.; Buchwald, S. L. *Chem. Sci.* **2011**, *2*, 27−50.
(15) Maiti, D.; Buchwald, S. L. *J. Org. Chem.* **2010**, *75*, 1791−1794.
(16) Salvi, L.; Davis, N. R.; Ali, S. Z.; Buchwald, S. L. *Org. Lett.* **2011**, *14*, 170−173.
(17) Lakowicz, J. R. *Principles of Fluorescence Spectroscopy*; 3rd ed.; Springer Science+Business Media: New York, 2006.
(18) Tverskoy, O.; Rominger, F.; Peters, A.; Himmel, H.-J.; Bunz, U. H. F. *Angew. Chem., Int Ed.* **2011**, *50*, 3557−3560.
(19) Lindner, B. D.; Engelhart, J. U.; Tverskoy, O.; Appleton, A. L.; Rominger, F.; Peters, A.; Himmel, H.-J.; Bunz, U. H. F. *Angew. Chem. Int Ed.* **2011**, *50*, 8588−8591.
(20) Lindner, B. D.; Engelhart, J. U.; Märken, M.; Tverskoy, O.; Appleton, A. L.; Rominger, F.; Hardcastle, K. I.; Enders, M.; Bunz, U. H. F. *Chem.—Eur. J.* **2012**, *18*, 4627−4633.
(21) Schleyer, P. v. R.; Maerker, C.; Dransfeld, A.; Jiao, H.; Hommes, N. J. R. v. E. *J. Am. Chem. Soc.* **1996**, *118*, 6317−6318.
(22) Chen, Z.; Wannere, C. S.; Corminboeuf, C.; Puchta, R.; Schleyer, P. v. R. *Chem. Rev.* **2005**, *105*, 3842−3888.
(23) Stanger, A. *J. Org. Chem.* **2005**, *71*, 883−893.
(24) Fallah-Bagher-Shaidaei, H.; Wannere, C. S.; Corminboeuf, C.; Puchta, R.; Schleyer, P. v. R. *Org. Lett.* **2006**, *8*, 863−866.
(25) TURBOMOLE V6.3.1 2011, a development of University of Karlsruhe and Forschungszentrum Karlsruhe GmbH, 1989−2007, TURBOMOLE GmbH, since 2007; available from http://www.turbomole.com.
(26) Gaussian 09, Revision B.01: Frisch, M. J.; Trucks, G. W.; Schlegel, H. B.; Scuseria, G. E.; Robb, M. A.; Cheeseman, J. R.; Scalmani, G.; Barone, V.; Mennucci, B.; Petersson, G. A.; Nakatsuji, H.; Caricato, M.; Li, X.; Hratchian, H. P.; Izmaylov, A. F.; Bloino, J.; Zheng, G.; Sonnenberg, J. L.; Hada, M.; Ehara, M.; Toyota, K.; Fukuda, R.; Hasegawa, J.; Ishida, M.; Nakajima, T.; Honda, Y.; Kitao, O.; Nakai, H.; Vreven, T.; Montgomery, J. A., Jr.; Peralta, J. E.; Ogliaro, F.; Bearpark, M.; Heyd, J. J.; Brothers, E.; Kudin, K. N.; Staroverov, V. N.; Keith, T.; Kobayashi, R.; Normand, J.; Raghavachari, K.; Rendell, A.; Burant, J. C.; Iyengar, S. S.; Tomasi, J.; Cossi, M.; Rega, N.; Millam, J. M.; Klene, M.; Knox, J. E.; Cross, J. B.; Bakken, V.; Adamo, C.; Jaramillo, J.; Gomperts, R.; Stratmann, R. E.; Yazyev, O.; Austin, A. J.; Cammi, R.; Pomelli, C.; Ochterski, J. W.; Martin, R. L.; Morokuma, K.; Zakrzewski, V. G.; Voth, G. A.; Salvador, P.; Dannenberg, J. J.; Dapprich, S.; Daniels, A. D.; Farkas, O.; Foresman, J. B.; Ortiz, J. V.; Cioslowski, J.; , and Fox, D. J. Gaussian, Inc., Wallingford CT, 2010.
(27) Wu, J. I.; Wannere, C. S.; Mo, Y.; Schleyer, P. v. R.; Bunz, U. H. F. *J. Org. Chem.* **2009**, *74*, 4343−4349.
(28) Payne, M. M.; Parkin, S. R.; Anthony, J. E. *J. Am. Chem. Soc.* **2005**, *127*, 8028−8029.
(29) Brédas, J. L.; Calbert, J. P.; da Silva Filho, D. A.; Cornil, J. *Proc. Natl. Acad. Sci. U.S.A.* **2002**, *99*, 5804−5809.